

Article

# Wet Peroxide Oxidation of Paracetamol Using Acid Activated and Fe/Co-Pillared Clay Catalysts Prepared from Natural Clays

Adriano Santos Silva <sup>1,2</sup>, Marzhan Seitovna Kalmakhanova <sup>3</sup> ,  
Bakytgul Kabykenovna Massalimova <sup>3</sup> , Juliana G. Sgorlon <sup>4</sup>, Jose Luis Diaz de Tuesta <sup>1,2,\*</sup>   
and Helder Teixeira Gomes <sup>1,2,\*</sup> 

<sup>1</sup> Centro de Investigação de Montanha (CIMO), Instituto Politécnico de Bragança, 5300-253 Bragança, Portugal

<sup>2</sup> Laboratory of Separation and Reaction Engineering—Laboratory of Catalysis and Materials (LSRE-LCM), Faculdade de Engenharia, Universidade do Porto, 4200-465 Porto, Portugal

<sup>3</sup> Department of Chemistry and Chemical Engineering, M.Kh. Dulati Taraz State University, Tole bi 63, 080012 Taraz, Kazakhstan

<sup>4</sup> Universidade Tecnológica Federal do Paraná, R. Marcílio Dias, 635-Jardim Paraiso, Apucarana PR 86812-460, Brasil

\* Correspondence: jl.diazdetuesta@ipb.pt (J.L.D.d.T.); htgomes@ipb.pt (H.T.G.)

Received: 29 July 2019; Accepted: 19 August 2019; Published: 22 August 2019



**Abstract:** Many pharmaceuticals have been recently identified at trace levels worldwide in the aquatic environment. Among them, the highly consumed paracetamol (PCM), an analgesic and antipyretic drug, is largely being accumulated in the aquatic environment due to inefficient removal by conventional sewage treatment plants. This work deals with the treatment of PCM, used as a model pharmaceutical contaminant of emerging concern, by catalytic wet peroxide oxidation using clay-based materials as catalysts. The catalysts were prepared from natural clays, extracted from four different deposits using acid-activated treatment, calcination, and pillarization with Fe and Co. Pillared clays show the highest catalytic activity owing to the presence of metals, allowing to remove completely the PCM after 6 h under the following operating conditions:  $C_{PCM} = 100 \text{ mg L}^{-1}$ ,  $C_{H_2O_2} = 472 \text{ mg L}^{-1}$ ,  $C_{cat} = 2.5 \text{ g L}^{-1}$ , initial pH = 3.5 and  $T = 80 \text{ }^\circ\text{C}$ . The prepared materials presented high stability since leached iron was measured at the end of reaction and found to be lower than  $0.1 \text{ mg L}^{-1}$ .

**Keywords:** advanced oxidation process; wastewater treatment; contaminants of emerging concern; pharmaceuticals; environmental catalysis

## 1. Introduction

In recent years, and especially after the development of sophisticated analytical techniques, many pharmaceuticals have been identified at trace levels ( $\text{ng L}^{-1}$ – $\text{mg L}^{-1}$ ) worldwide in the aquatic environment [1]. Municipal wastewater treatment plants (WWTPs) are considered the main sources of these pollutants as they are not generally prepared to deal with these complex substances, and thus they are usually ineffective in their complete removal [1–4]. Despite the low concentration of drugs contained in those effluents, their continuous input constitutes an important environmental threat, given their persistence and hazardous nature [5–8].

The presence of pharmaceuticals, even in trace concentrations, affects the quality of water and constitutes a risk of toxicity for the ecosystems and living organisms. A number of effects, such as the development of antibiotic-resistant bacteria in the aquatic environment [7], fish reproduction changes due to the presence of estrogenic compounds [5] and specific inhibition of photosynthesis in algae

caused by  $\beta$ -blockers have been reported [6]. Moreover, according to most recent works, the biological effects of low-dose complex micropollutant mixtures are still underestimated [8]. This also constitutes a public health problem since pharmaceuticals have even been found in drinking water supplies [9]. Consequently, new regulation for micropollutant discharge and monitoring has recently started in different countries [10,11].

So far, there are no legal requirements for the discharge of these ubiquitous and biologically active substances, but this scenario is expected to change in the next few years. The European Union (EU) has recently approved a watch list of 17 substances, among them 7 pharmaceuticals, for their monitoring in the EU-water basins (Decision 2015/495/EC) [11]. Those substances showing a significant risk will be potentially listed as priority pollutants.

Among pharmaceutical compounds that can cause pollution of water, paracetamol (PCM) deserves particular attention, since it has recently been discovered as a potential pollutant of waters [12–16]. PCM is an analgesic and antipyretic drug that is largely accumulated in the aquatic environment due to its inefficient removal by conventional sewage treatment plants, also representing an important material for the industry of manufacturing of azo dyes and photographic chemicals [17]. The concern about the environmental impact of its biodegradation products has been growing, because of its hepatotoxicity and the possibility of those products to be toxic or hazardous in trace amounts [12]. It is clear that optimization of WWTPs by including efficient tertiary treatments to create an effective barrier to micropollutants emission is a social responsibility and a task of high priority. Successful results have been reported at the laboratory scale for the elimination of a wide range of pharmaceuticals by Fenton-like processes [18]. The Fenton process has been successfully tested in the treatment of pharmaceutical compounds [18,19]. However, the Fenton process produces large amounts of ferrous iron sludge, and an additional process is required. The immobilization of iron onto a solid support in the so-called catalytic wet peroxide oxidation (CWPO) has proved to be an interesting strategy to overcome those limitations. Although this technology represents an interesting alternative, it has been scarcely studied so far for micropollutants abatement [18,20]. Clays play a prominent role as a catalyst in the field of organic pollutants removal by CWPO [21–25]. In this regard, natural clays can be chemically modified to increase their performance by different methods, such as activation or pillarization. On the one hand, the acid activation of a clay consists of the release of metal cations from the layered structure of the clay, creating Lewis and Brønsted sites and leading to an increment of the surface area [26,27]. On the other hand, the process of pillarization consists of the intercalation of the cations present in a previously selected pillaring solution into the interlayer space of the clays, which involves the natural substitution of exchangeable cations present between the sheets of clays [28]. Both activation and pillarization methods can lead to an increase in the catalytic activity of the clays, but clay-based materials have not been assessed in the treatment of contaminants of emerging concern, such as pharmaceutical compounds.

This work deals with the CWPO of PCM, used as pharmaceutical model compound, with modified clay-based catalysts prepared from natural clays extracted from the deposits of four different regions of Kazakhstan. PCM removal and mineralization is addressed with natural, acid-activated, calcined and pillared clays.

## 2. Results and Discussion

### 2.1. Characterization of Materials

#### 2.1.1. Textural Properties

The nitrogen adsorption isotherms at 77 K obtained for the prepared clay-based materials are depicted in Figure 1. All materials show similar  $N_2$  sorption isotherms, classified as Type II, as typically found for non-macroporous adsorbents according to the current IUPAC classification [29], following the revisions of 1985 IUPAC recommendations on physisorption isotherms. All samples also show a similar hysteresis loop (only shown in Figure 1 for the KO-PILC sample), classified as Type H3 by IUPAC [29].

Loops of this type are attributed to non-rigid aggregates of plate-like particles (e.g., certain clays) but also to materials with pore networks consisting of macropores not completely filled with condensate. As can be observed, the KO-PILC sample is able to adsorb more nitrogen on its surface when compared to the other pillared clays shown in Figure 1a. However, there are no significant differences between the Kokshetau-based clays prepared from KO-N shown in Figure 1b. The acid activated clay (KO-A) is able to adsorb more nitrogen, resulting in the sample with the best textural properties (Table 1), namely the highest BET surface area and total pore volume ( $28 \text{ m}^2 \text{ g}^{-1}$  and  $94.6 \text{ mm}^3 \text{ g}^{-1}$ , respectively). The development of porosity by the acid activation of natural clays could be expected to be higher than observed, but natural clays used in this work possess high amount of impurities in the form of quartz (>45%), limiting the porous development [21]. The pillarization of these clays does not result in an increment of the specific surface area or pore volume, also as a consequence of the quartz content of the natural clays employed, as discussed in previous works [21].

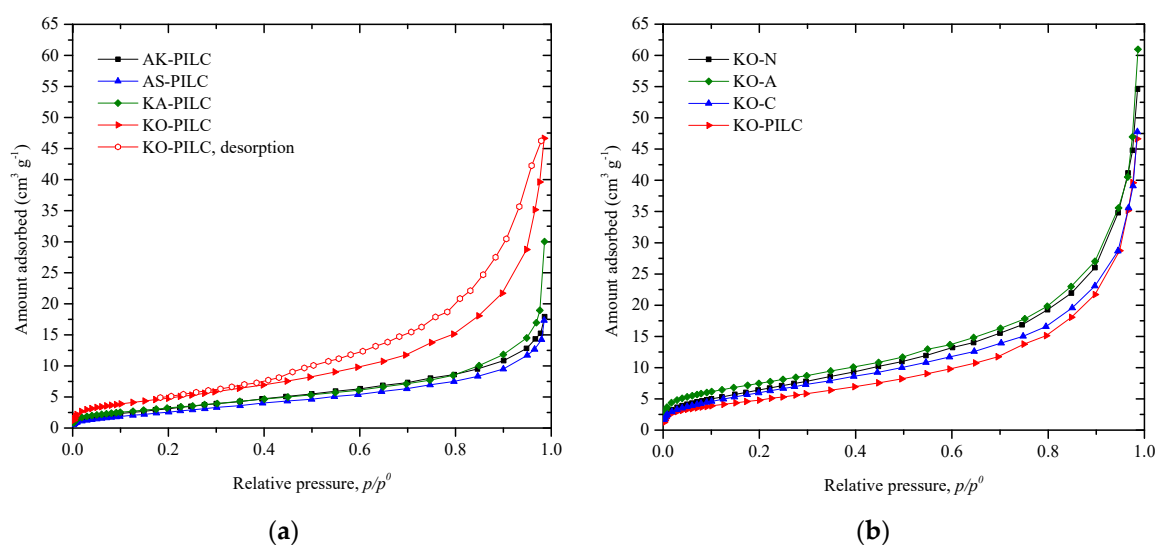


**Figure 1.**  $\text{N}_2$  adsorption isotherms at 77 K of (a) pillared clays and (b) Kokshetau-based clays.

**Table 1.** Textural properties of the clay-based samples.

Sample	$S_{\text{BET}}$ ( $\text{m}^2 \text{ g}^{-1}$ )	$V_{\text{Total}}$ ( $\text{mm}^3 \text{ g}^{-1}$ )
KO-N	26	69.2
KO-A	28	94.6
KO-C	24	74.0
KO-PILC	19	72.3
AK-PILC	13	27.8
AS-PILC	11	22.1
KA-PILC	13	46.6

### 2.1.2. Surface Composition

Figure 2 gathers the XRD diffractograms of the Kokshetau and Karatau based samples. As observed, both clays present the typical reflection of montmorillonite [30]. As the samples were provided from natural deposits, it was expected that its crystal compositions were formed not only by one clay mineral, but by multiple phases. In this sense, it is also possible to find traces of saponite [31], kaolinite [32] and muscovite [33] in the sample KA-N. The material KO-N also evidences the presence of kaolinite [31]. Both natural samples also present a peak at  $26.7^\circ$  related to the presence of impurities of quartz ( $\text{SiO}_2$ ) [34,35]. Even knowing that the natural clays present not only montmorillonite in its crystal composition, the intensities of the peaks in the positions referred to this mineral are higher than the intensities assigned to the other phases, suggesting that the clays are mainly composed by

montmorillonite. Therefore, both natural clays can be classified as bentonite, which is the denomination given to the class of clays composed by a mixture of different clay minerals, with a major composition of montmorillonite [36]. It is possible to observe that the signal for SiO<sub>2</sub> and metal oxides such as aluminum oxide and iron (III) oxide decreased in the diffractogram obtained with KO-A when compared to that of KO-N. This can be explained by the fact that the acid treatment washes partially the impurities of SiO<sub>2</sub> from the natural clay, also leaching a small amount of the metals. In the diffractogram of KO-C, the signals attributed to iron (III) and alumina oxides were the same as those obtained in the diffractogram of KO-N, and the signal attributed to SiO<sub>2</sub> had a small decrease. Finally, in the diffractogram of KO-PILC, the signal for iron (III) oxide was significantly higher than in that observed for the natural sample KO-N, confirming the successful incorporation of iron in the clay structure. For the pillared sample KA-PILC it is possible to observe the decrease for the signal of the SiO<sub>2</sub> impurities, and that the signal of the iron (III) oxide increased significantly, putting in evidence the incorporation of iron in the material. In fact, the signal attributed to iron (III) oxide in this sample was higher than in the others.

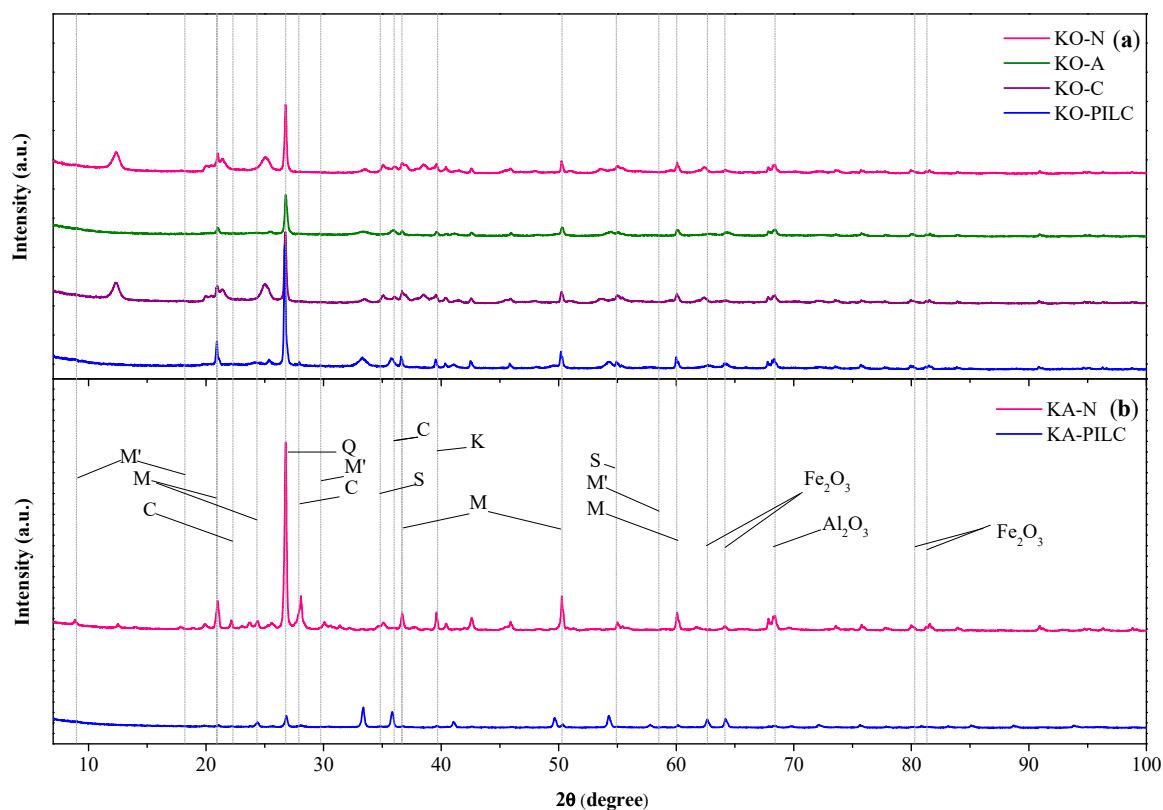


**Figure 2.** XRD spectra of (a) Kokshetau and (b) Karatau based clays (M = Montmorillonite, S = Saponite, K = Kaolinite, M' = Muscovite, C = Calcite, Q = Quartz).

Besides all the differences between the signals in both diffractograms of the Kokshetau and Karatau samples, it is interesting to observe that the signal for montmorillonite, kaolinite, saponite, and muscovite did not change significantly in the different samples. This suggests that the main structure of the clay is stable, although passing through some structural changes [37].

The FT-IR spectra obtained from the analysis of all the natural clays and of the corresponding prepared pillared clay samples are depicted in Figure 3. As can be observed, the natural clays from Akzhar, Asa and Karatau (AK-N, AS-N and KA-N, respectively) show a band close to 1450 cm<sup>-1</sup>. As detected in a previous work [21], this band is due to the presence of calcite in the natural materials, disappearing after the pillarization process because of the exchange between calcium and the pillaring metals [38]. The band at 870 cm<sup>-1</sup> appearing in the natural samples can be ascribed to the Al–Mg–OH

bending vibrations. The disappearance of this band in the spectra obtained with the pillared samples is due to the fracture of these bonds [39] and can also be ascribed to the exchange of the cation  $Mg^{2+}$  by the pillaring procedure. The bands observed in the range of  $1000\text{--}1025\text{ cm}^{-1}$  is present in the spectra of all the samples, and represent the stretching vibrations of the Si–O bond group [40]. The band observed in the range of wavenumbers from  $776\text{ to }780\text{ cm}^{-1}$  is attributed to the presence of the quartz impurity [41]. The band observed close to  $530\text{ cm}^{-1}$  is associated with the bending vibrations of the group Si–O–Mg [34]. At  $470\text{ cm}^{-1}$  it is also possible to observe another band that is related to the presence of bending vibrations of Si–O–Fe bonds [42,43], which is present in all samples (pillared and natural) as a consequence of the presence of iron in natural clays, as reported previously [21].

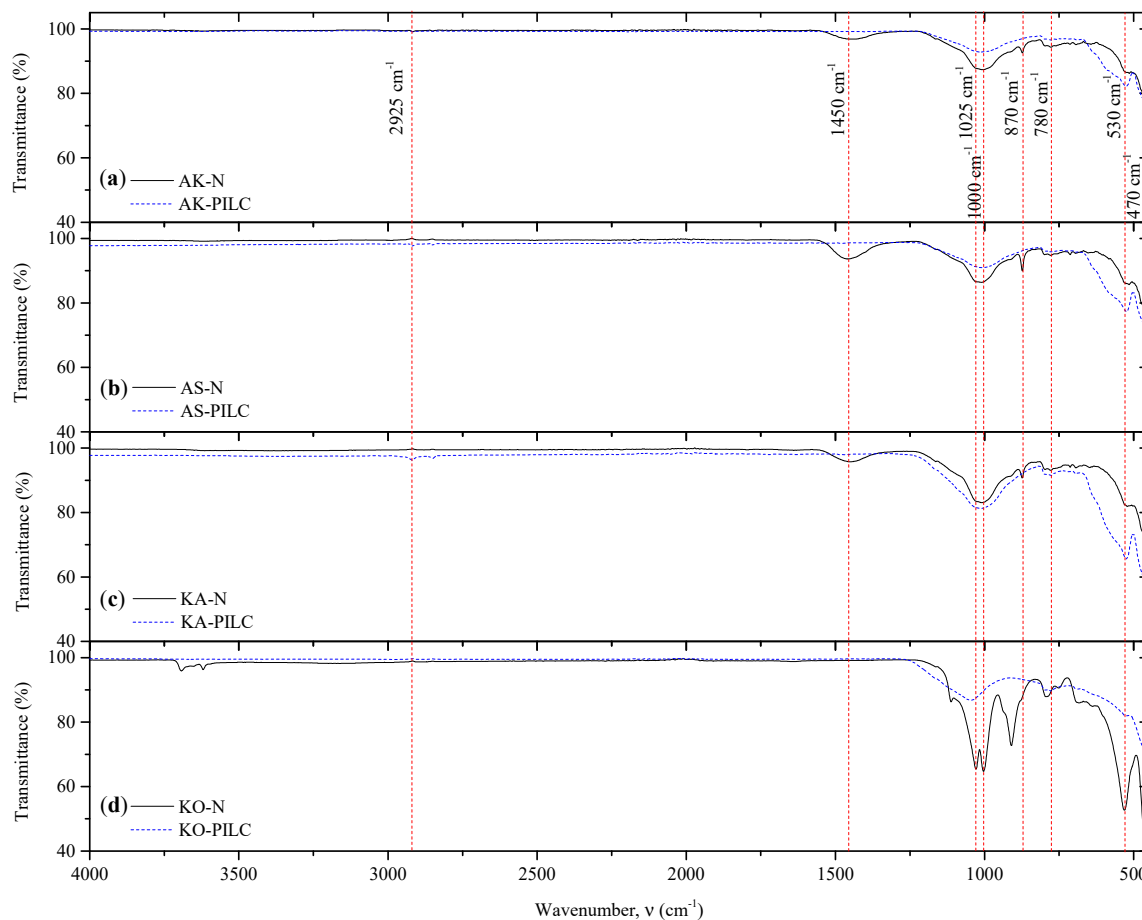


**Figure 3.** FT-IR spectra of (a) Akzhar, (b) Asa, (c) Karatau and (d) Kokshetau based clays in natural and pillared form.

### 2.1.3. Acid-Base Characterization

The acid–base properties and the pH of the point of zero charge ( $pH_{PZC}$ ) of the clay-based materials are gathered in Table 2. It can be concluded that all the clay-based materials possess a neutral character around 7–8 of  $pH_{PZC}$ .

**Table 2.** Acid-base characterization of the clay-based materials.

Sample	$pH_{PZC}$	Acidity ( $\mu\text{mol g}^{-1}$ )	Basicity ( $\mu\text{mol g}^{-1}$ )
KO-N	7.8	350	245
KO-A	7.2	987	614
KO-C	8.0	338	270
KO-PILC	7.4	950	652
AK-PILC	7.2	812	538
AS-PILC	7.6	475	372
KA-PILC	7.4	687	627

Among the modified Kokshetau clays, it is possible to observe that the KO-PILC and the KO-A possess more than 950 and 600  $\mu\text{mol g}^{-1}$  respectively of acidic and basic functionalities, whereas the natural and the calcined samples (KO-N and KO-C, respectively) present an acidity and a basicity lower than 350 and 270  $\mu\text{mol g}^{-1}$ , respectively. Thus, the acidity and basicity are increased up to three times after the pillarization or acid activation treatments of the natural clay (KO-N). Both treatments lead to similar acidity (950 and 987  $\mu\text{mol g}^{-1}$  for KO-PILC and KO-A, respectively) and basicity (652 and 614  $\mu\text{mol g}^{-1}$  for KO-PILC and KO-A, respectively), concluding that no significant changes are found in this sense regarding the treatment process.

The pillared clays prepared from the different natural clays also present differences between them. The pillared clay prepared from the Kokshetau natural clay (KO-PILC) presents the highest acidity and basicity (950 and 652  $\mu\text{mol g}^{-1}$ , respectively). The acidity of pillared clays was found to decrease in the following order: KO-PILC (950  $\mu\text{mol g}^{-1}$ ) > AK-PILC (812  $\mu\text{mol g}^{-1}$ ) > KA-PILC (687  $\mu\text{mol g}^{-1}$ ) > AS-PILC (475  $\mu\text{mol g}^{-1}$ ), whereas the value of the basicity diminishes as follow: KO-PILC (652  $\mu\text{mol g}^{-1}$ ) > KA-PILC (627  $\mu\text{mol g}^{-1}$ ) > AK-PILC (538  $\mu\text{mol g}^{-1}$ ) > AS-PILC (372  $\mu\text{mol g}^{-1}$ ).

The acidity and basicity of a catalyst play an important role in the decomposition of  $\text{H}_2\text{O}_2$  and in the CWPO of pollutants, as observed in previous works related to the CWPO of phenol compounds with carbon-based catalysts [44]. In works related to the CWPO with clay-based catalysts, a correlation between the acidity of the catalysts and their performance in the oxidation process has also been observed [22–24]. However, the cited previous studies used a qualitative methodology, based on FTIR analysis of base compound-saturated clays, and acidity and basicity were not quantified.

## 2.2. CWPO of Paracetamol

Figure 4 shows the relative concentration of PCM,  $\text{H}_2\text{O}_2$  and TOC upon reaction time with the non-pillared clays prepared from the natural clay extracted from the Kokshetau deposit, viz. KO-N, KO-C and KO-A. As observed, all materials are catalytic active in the CWPO of PCM and allow to remove more than 34% of PCM after 24 h, whereas the non-catalytic run lead to a conversion of 20% after 24 h of reaction time at same operating conditions. The removal of the pollutant with the different clay-based materials reach values between 34% and 48% with a low consumption of  $\text{H}_2\text{O}_2$  (20%–26%) with the natural, calcined and acid activated clays after 24 h of reaction and same operational conditions. The TOC abatement reached similar conversions (23%–29% after 24 h of reaction time) to those found for  $\text{H}_2\text{O}_2$ . It is also possible to observe that the mineralization reached with the clay-based materials is higher when compared to the non-catalytic run (9% after 24 h of reaction). Slight differences of the catalytic activity in the CWPO of PCM can be found for the non-pillared clays. The lowest catalytic activity was found for the calcined sample (KO-C), which can be explained by the lowest BET surface area of this material and the highest  $pH_{PZC}$  value [44]. The higher conversions of PCM,  $\text{H}_2\text{O}_2$  and TOC obtained with the KO-A sample were ascribed to the highest values of acidity and basicity, as well as to its textural properties when compared to the other samples. Regarding the TOC removal results given in Figure 4c, it is possible to observe in the right axis that the oxidized intermediates produced may be refractory, since the TOC derived from PCM (TOC contribution determined as the subtraction of the theoretical TOC contribution of PCM from the measured TOC), increased continuously during

the time evaluated in the experiments. Catalytic performance should be improved in order to obtain the complete removal of the model pollutant and, in addition, a catalyst able to remove some of the oxidized intermediates products. This endeavor was the main target that justified the preparation of the pillared catalysts.

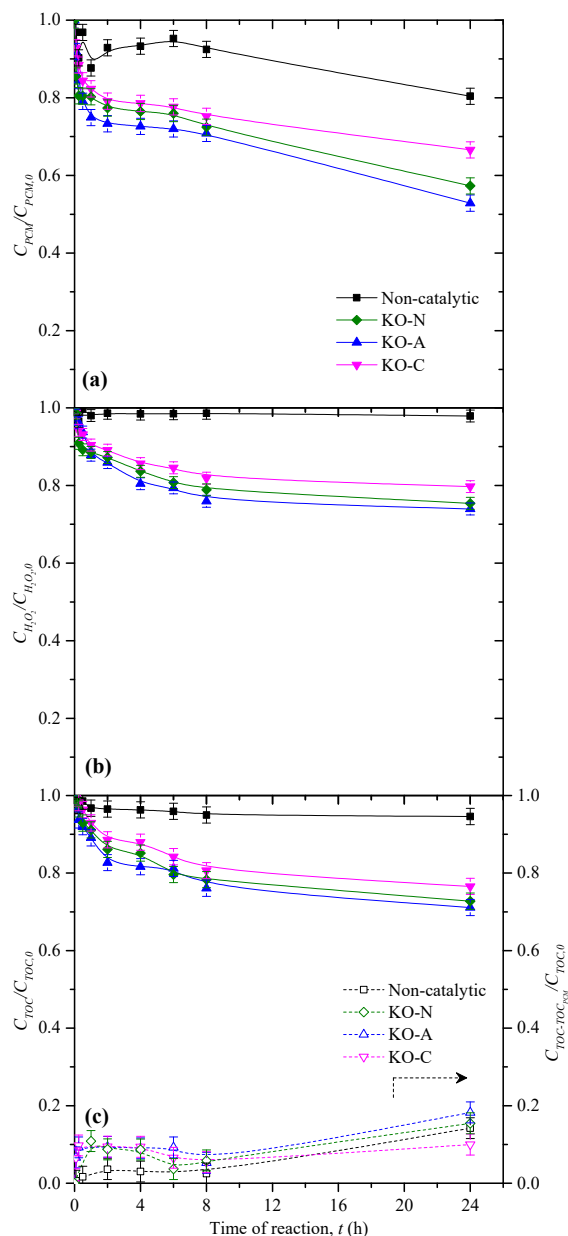


**Figure 4.** Profiles of the relative concentrations of (a) paracetamol (PCM), (b)  $H_2O_2$  and (c) TOC during the catalytic wet peroxide oxidation (CWPO) of PCM with the non-pillared clays prepared from the natural clay extracted from the Kokshetau deposit. Operating conditions:  $C_{PCM} = 100 \text{ mg L}^{-1}$ ,  $C_{H_2O_2} = 472 \text{ mg L}^{-1}$ ,  $C_{cat} = 2.5 \text{ g L}^{-1}$ , initial pH = 3.5 and  $T = 80 \text{ }^\circ\text{C}$ .

The results of the CWPO of PCM obtained with the pillared clays prepared from the four different deposits considered in this work are represented in Figure 5. As observed, all pillared materials show higher catalytic activity when compared to the non-pillared Kokshetau samples previously shown. In fact, a significant difference can be observed between the pillared sample (KO-PILC) and the non-pillared samples, since the KO-PILC leads to a complete removal of PCM after 6 h. In addition, a mineralization of 79% is achieved with KO-PILC, whereas TOC abatement reached only 29% with

the non-pillared samples. The highest catalytic activity of the KO-PILC in the CWPO of PCM when compared to the other Kokshetau samples can be explained only as a consequence of the presence of cobalt and iron, since the acidic and textural properties are similar to the non-pillared samples, evidencing that those metals are working as the main active phases in the catalyst. As can also be observed, all pillared materials present higher conversions of PCM,  $H_2O_2$  and TOC (more than 78%, 71% and 28% after 8 h of reaction time, respectively) when compared to the non-pillared samples (34%, 20% and 23% at the same operating conditions, respectively). Two pillared samples (KO-PILC and KA-PILC) allow to remove completely the PCM after 6 h of reaction. Among them, KO-PILC show the highest catalytic activity in the CWPO of PCM, leading to the highest removal of TOC (68% after 8 h of reaction time). This can be ascribed to the highest BET surface area and to the highest amount of acidic and basic functionalities of the material, as well as to the highest content of iron (9%) of the natural clays, as observed in a previous work [21].

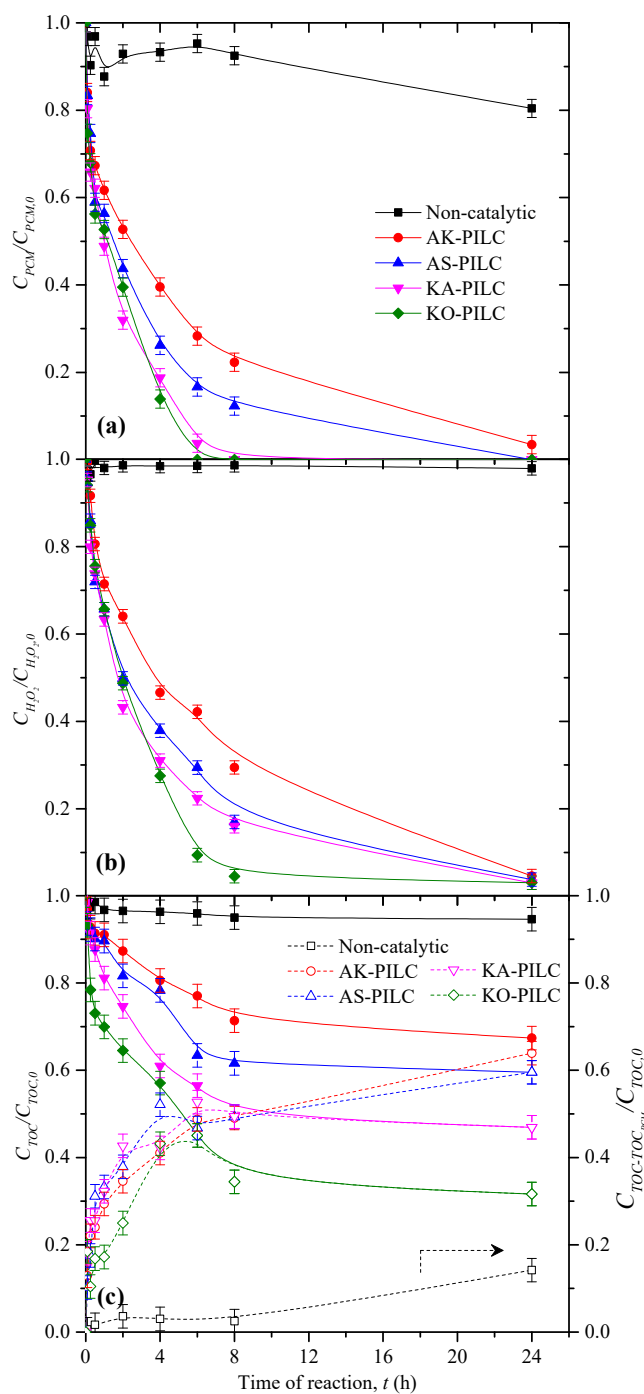


**Figure 5.** Profile of relative concentrations of (a) PCM, (b)  $H_2O_2$  and (c) TOC during the CWPO of PCM with pillared clays. Operating conditions:  $C_{PCM} = 100 \text{ mg L}^{-1}$ ,  $C_{H_2O_2} = 472 \text{ mg L}^{-1}$ ,  $C_{cat} = 2.5 \text{ g L}^{-1}$ , initial pH = 3.5 and  $T = 80 \text{ }^\circ\text{C}$ .

As can be seen, the TOC profile free of the TOC contribution of paracetamol (expressed as  $C_{TOC-TOC_{PCM}}$  and represented as open symbols in Figure 5c) reaches a maximum value close to 5 h, evidencing that some of the oxidized intermediates are further oxidized during the CWPO of PCM. After 6 h, when PCM disappeared, the profile is aligned with the measured TOC values and a partially decrease of the oxidized intermediates is then observed. In this work, the analysis of the different aliquots taken from the reaction media were done by HPLC, as described in the methodology section. However, calibrated compounds (*p*-nitrophenol, *p*-nitrocatechol, hydroquinone, *p*-benzoquinone, resorcinol, pyrocatechol, phenol and *trans, trans*-muconic acid) were not identified during the CWPO

experiments, but a decrease of the pH during the experiments of CWPO was always observed, reaching values of 3.49, 3.35, 3.21, 3.18, 3.07, 3.00, 2.85 and 2.68 after 24 h in the non-catalytic run with the KO-C, KO-N, KO-A, AK-P, AS-P, KA-P and KO-P, respectively. This evidence supports the formation of carboxylic acid groups as oxidized intermediate compounds during the CWPO of PCM experiments. The material with highest performance (KO-PILC) led to the minimal pH (2.68) observed after 24 h, meaning that a high extent of oxidation was reached.

To the best of our knowledge, there is no other work that uses modified clays in the CWPO of PCM, but it is possible to find studies regarding the degradation of PCM by Fenton-like process [20,45,46]. Velichkova et al. [20] obtained the complete removal of PCM after 4 h using a nanostructured maghemite powder catalyst under the following operating conditions:  $C_{PCM} = 100 \text{ mg L}^{-1}$ ,  $C_{H_2O_2} = 28 \text{ mmol L}^{-1}$ ,  $C_{cat} = 6 \text{ g L}^{-1}$ , initial pH = 2.6 and  $T = 60 \text{ }^\circ\text{C}$ . Similar results have been achieved in our work, since a complete removal of PCM is achieved using the lowest quantities of catalyst and hydrogen peroxide, despite a slightly higher temperature. Similar values of mineralization were also found in this work. Alalm et al. [45] achieved the complete removal of PCM after 1 h by photo-Fenton ( $\text{FeSO}_4 \cdot 7\text{H}_2\text{O}$ ) at the following operating conditions:  $C_{PCM} = 100 \text{ mg L}^{-1}$ ,  $C_{H_2O_2} = 1500 \text{ mg L}^{-1}$ ,  $C_{cat} = 0.5 \text{ g L}^{-1}$  and initial pH = 3.0. In this case, PCM was removed quickly than in our study, but using an additional support of energy (the UV light) and adding a quantity of  $\text{H}_2\text{O}_2$  considerably higher than the stoichiometric amount used in our work. In addition, the use of a homogeneous catalyst requires an additional process to recover the catalyst. In this previous study, the TOC or identified oxidized intermediates was not followed. Trovó et al. [46] also studied the photo-Fenton ( $\text{FeSO}_4 \cdot 7\text{H}_2\text{O}$ ) of PCM ( $C_{PCM} = 50 \text{ mg L}^{-1}$ ,  $C_{H_2O_2} = 120 \text{ mg L}^{-1}$ ,  $C_{cat} = 0.05 \text{ mM}$  and initial pH = 2.5). Under those conditions, PCM was completely removed after 2 h. However, an additional source of energy and a homogeneous catalyst was used. A mineralization of 79% was achieved after 5 h of reaction, but the oxidized intermediates were not studied.

The adsorption and the homogeneous catalytic contribution in the removal of PCM was addressed by pure adsorption runs on the clays and by the determination of the leaching of iron from the materials during the CWPO experiments (Figure 6). PCM removal achieved in pure adsorption runs reached values from 4% to 18% after 24 h of contact time, values considerably lower when compared to the conversion of PCM obtained in the CWPO runs after 8 h of reaction, as also represented in Figure 6. This evidences that PCM is disappeared during CWPO runs because of the oxidation, instead of adsorption, since its contribution is poor in comparison with oxidation.

The concentration of iron determined after the experiments of CWPO was found to be lower than the limit concentration of  $2 \text{ mg L}^{-1}$  of iron in water courses, established by EU directives for treated water to be discharged into natural receiving water bodies. Curiously, the largest values of leached iron concentration were found with the natural and with the calcined materials (KO-N and KO-C, respectively). Iron coming from these materials is due to the iron content that is presented in the pristine material (9%) [21]. Among the non-pillared materials, the acid activated clay (KO-A) does not show leached iron precisely because of the treatment with the acid. Considering the values of the leaching of iron obtained with the non-pillared clays it is possible to consider that the homogeneous contributions are negligible. In fact, the maximum value of leached iron concentration among pillared clays was found with AK-PILC ( $0.097 \text{ mg L}^{-1}$ ) that showed the lowest catalytic activity in the CWPO of PCM. In addition, taking into account the theoretical maximum value of iron that is possible to observe in the media of reaction from the iron incorporated during the pillaring process (more than  $800 \text{ mg L}^{-1}$ ), it is also possible to conclude that the materials show high stability (less than 0.015% of the iron present in the clays was leached).

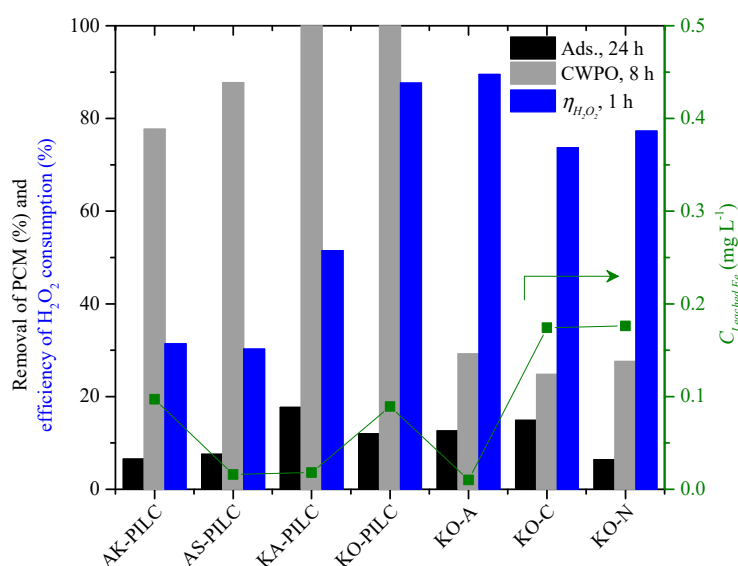


**Figure 6.** Pollutant removal by CWPO and by pure adsorption after 8 and 24 h, respectively; and  $H_2O_2$  consumption efficiency and leached iron after 1 and 24 h of time of reaction, respectively in CWPO runs. Operating conditions:  $C_{PCM} = 100 \text{ mg L}^{-1}$ ,  $C_{H_2O_2} = 472 \text{ mg L}^{-1}$ ,  $C_{cat} = 2.5 \text{ g L}^{-1}$ , initial pH = 3.5 and  $T = 80 \text{ }^\circ\text{C}$ .

### 3. Materials and Methods

#### 3.1. Reactants and Materials

Natural clays were supplied from four different deposits of Kazakhstan, viz. Akzhar, Asa, Karatau and Kokshetau (AK-N, AS-N, KA-N and KO-N samples, respectively). Acetic acid glacial (99.8%) and sodium acetate (98%) were obtained from Fischer Chemical and used in the buffer solution prepared for washing the clays. Iron (III) chloride hexahydrate (99%) and cobalt (II) chloride hexahydrate (99%) supplied from Aldrich and Fischer Chemical respectively, were used to prepare the pillaring solution. 4-acetamidophenol (paracetamol, 98%), obtained from Alfa Aesar, was used as model pollutant. Hydrogen peroxide (30% *w/v*), supplied by Fisher Chemical, was used as an oxidant. For analytical techniques, titanium (IV) oxysulfate (99.99%), sulfuric acid (98%), anhydrous sodium sulphite (98%), ortho-phosphoric acid (85%), acetonitrile (99.95%) and iron (II) chloride tetrahydrate (99%), obtained from Aldrich, Labkem, Panreac, Riedel-de Haen, VWR and Sigma-Aldrich respectively, were used. Ultrapure water was used in the preparation of solutions.

#### 3.2. Preparation of Clay-Based Materials

Pillared clays were prepared using a pillaring solution that was prepared by dropwise addition of 0.5 M NaOH solution, at room temperature, to an aqueous solution of 0.5 M  $FeCl_3$  and 0.25 M  $CoCl_2$  to obtain a final solution with a molar ratio  $OH/(Fe + Co) = 2:1$ . Then, the pillaring solution was added into a 2 wt % natural clay suspension (natural clays were washed previously with a sodium acetate buffer solution). The resultant suspension was stirred at room temperature during 3 h, aged during 72 h and then the clay being recovered by filtration. The material was washed with water until the rinsing waters reach the natural pH, dried overnight at  $60 \text{ }^\circ\text{C}$  and calcined at  $600 \text{ }^\circ\text{C}$  during 5 h, resulting in AK-PILC, AS-PILC, KA-PILC, KO-PILC materials, obtained respectively from AK-N, AS-N, KA-N and KO-N samples. Additionally, one sample calcined at same conditions ( $600 \text{ }^\circ\text{C}$  for 5 h) was prepared from the KO-N in order to compare the effect of the calcination without the pillarization process, resulting in the sample KO-C. An acid activated clay was also prepared by immersing 3 g of KO-N in 150 mL of 4 M  $H_2SO_4$  at  $80 \text{ }^\circ\text{C}$  for 3 h to compare the effectiveness between pillared and acid-activated clays, resulting in the sample KO-A.

### 3.3. Techniques of Characterization

The textural properties of the materials were determined from N<sub>2</sub> adsorption–desorption isotherms at 77 K, obtained in a Quantachrome instrument NOVA TOUCH LX4 [47]. The specific surface area ( $S_{BET}$ ) was calculated using the BET method using the Quantachrome TouchWin™ software 1.21. The total pore volume ( $V_{Total}$ ) was considered at  $p/p^0 = 0.98$ . Fourier Transform Infrared (FT-IR) spectroscopy was performed with a Perkin Elmer FT-IR spectrophotometer UATR Two with a resolution of 1 cm<sup>-1</sup> and scan range of 4000 to 450 cm<sup>-1</sup> using the sample in powder solid state without further preparation. X-ray diffraction (XRD) analysis was performed in a PANalytical X'Pert PRO equipped with a X'Celerator detector and secondary monochromator (Cu K $\alpha$   $\lambda = 0.154$  nm; data recorded at a 0.017 degree step size). The crystallographic phases present were identified using a DEMO version of the HighScore software and the Crystallography Open Database.

The pH of the point of zero charge ( $pH_{PZC}$ ) was determined by pH drift tests, as described elsewhere [44]. Briefly, five NaCl (0.01 M) solutions were prepared as electrolyte with varying initial pH (in the range 2–10, using HCl and NaOH 0.1 M solutions). Samples of 0.05 g of pillared clays were contacted with 20 mL of each NaCl solution. The equilibrium pH of each suspension was measured after 48 h under stirring (320 rpm) at room temperature. The  $pH_{PZC}$  value was determined by intercepting the curve 'final pH vs initial pH' with the straight line 'final pH = initial pH'.

The concentrations of acidic and basic sites of the clays were determined following the methodology described in a previous work for carbon-based materials [44]. Briefly, the concentration of acidic sites was determined by adding 0.2 g of each clay to 25 mL of a 0.02 mol L<sup>-1</sup> NaOH solution. The resulting suspensions were left under stirring for 48 h at room temperature. After filtration, to remove the solid material, the unreacted OH<sup>-</sup> was titrated with a 0.02 mol L<sup>-1</sup> HCl solution. The initial concentration of acidic functionalities was then calculated by the difference between the amount of NaOH initially present in the suspension and the amount of NaOH determined by titration and dividing this value by the mass of material. The concentration of basic sites was determined in a similar way, this time by adding the carbon sample to a 0.02 mol L<sup>-1</sup> HCl solution and titration with a 0.02 mol L<sup>-1</sup> NaOH solution. Phenolphthalein was used as indicator in both titrations.

### 3.4. Oxidation Runs

Batch oxidation runs were carried out in a 250 mL well stirred round flask reactor equipped with a condenser and a temperature measurement thermocouple. An initial concentration of PCM of 100 mg L<sup>-1</sup> was considered to model wastewaters containing pharmaceutical compounds. The reactor was loaded with 100 mL of the PCM aqueous solution and heated by immersion in an oil bath at controlled temperature. Upon stabilization at the desired temperature (80 °C), the solution pH was adjusted to a previously chosen value by means of H<sub>2</sub>SO<sub>4</sub> solutions, and the experiments were allowed to proceed freely (not buffered). Then, the adequate quantity of 30% *w/v* H<sub>2</sub>O<sub>2</sub> solution was added in order to use the stoichiometric dosage of H<sub>2</sub>O<sub>2</sub> needed for PCM mineralization. Finally, the selected amount of catalyst was loaded (2.5 g L<sup>-1</sup>), being that moment considered as the initial reaction time,  $t_0 = 0$  h. All runs were conducted during 24 h. Pure adsorption runs were performed at the same operating conditions in the absence of H<sub>2</sub>O<sub>2</sub>, in order to compare with the pollutant removal obtained by CWPO experiments. Additionally, a blank experiment, in the absence of catalyst, was also carried out to observe the non-catalytic contribution to the drug degradation.

### 3.5. Analytical Techniques

Small aliquots were periodically withdrawn from the reactor, in order to be analysed by HPLC, TOC analysis and UV-Vis spectrophotometry, adapting methodologies described elsewhere [21,48]. PCM and its expected oxidized intermediate products (*p*-nitrophenol, *p*-nitrocatechol, hydroquinone, *p*-benzoquinone, resorcinol, pyrocatechol, phenol and *trans, trans*-muconic acid) were followed by using a Jasco HPLC system at a wavelength of 277 nm (UV-2075 Plus detector). For this purpose, a Kromasil

100-5-C18 column and  $0.65 \text{ mL min}^{-1}$  (PU-2089 Plus) of an A:B (10:90) mixture of acetonitrile (A) and sulfuric acid ( $\text{pH} = 3$ ) aqueous solution (B) were used. The concentration of  $\text{H}_2\text{O}_2$  was determined by adding the aliquot into a 5 mL volumetric flask containing 1 mL of  $\text{H}_2\text{SO}_4$  solution ( $0.5 \text{ mol L}^{-1}$ ) and 0.1 mL of  $\text{TiOSO}_4$ . The resulting mixture was diluted with distilled water and further analyzed at 405 nm using a T70 spectrometer of PG Instruments Ltd. (Lutterworth, United Kingdom). Total organic carbon (TOC) was determined using a TOC-L CSN analyser of Shimadzu (Kyoto, Japan).

Leached iron was determined only for the last sample, withdrawn from the reaction media, by atomic absorption spectroscopy (Varian SpectrAA 220).

#### 4. Conclusions

The preparation of clay-based materials by acid activation and by pillarization leads to an increase of the acidity character and of the specific surface area with respect to the corresponding natural clays. Despite this, the textural properties and the acidic functionalities were not found to affect significantly the catalytic activity of the clay materials in the CWPO of PCM, in opposition to the presence of Fe and Co in the prepared pillared clays. Whereas the maximum conversion of PCM achieved with non-pillared clays was 35% after 24 h, a complete removal of PCM was achieved with the Fe/Co-pillared clays under following conditions:  $C_{\text{PCM}} = 100 \text{ mg L}^{-1}$ ,  $C_{\text{H}_2\text{O}_2} = 472 \text{ mg L}^{-1}$ ,  $C_{\text{cat}} = 2.5 \text{ g L}^{-1}$ , initial  $\text{pH} = 3.5$  and  $T = 80 \text{ }^\circ\text{C}$ . The acid activated clays presented a higher specific surface area and similar acidity character when compared to the pillared clays, but less catalytic activity in the CWPO process, supporting the conclusion that Fe and Co are responsible for the high activity shown by the pillared clays. At the tested conditions, the iron anchored in the clays as pillars was found to be stable since non-significant leaching of the iron was observed.

**Author Contributions:** Conceptualization: A.S.S., J.L.D.d.T. and H.T.G.; investigation: A.S.S. and M.S.K.; writing—original draft preparation: A.S.S. and J.L.D.d.T.; writing—review: H.T.G.; supervision: J.L.D.d.T. and H.T.G.; resources: H.T.G., J.L.D.d.T., M.S.K. and B.K.M.

**Funding:** This work is a result of the Project “AIProcMat@N2020—Advanced Industrial Processes and Materials for a Sustainable Northern Region of Portugal 2020”, with the reference NORTE-01-0145-FEDER-000006, supported by Norte Portugal Regional Operational Programme (NORTE 2020), under the Portugal 2020 Partnership Agreement, through the European Regional Development Fund (ERDF); the Associate Laboratory LSRE-LCM—UID/EQU/50020/2019—funded by national funds through FCT/MCTES (PIDDAC); and CIMO (UID/AGR/00690/2019) through FEDER under Program PT2020.

**Conflicts of Interest:** The authors declare no conflict of interest.

#### References

1. Luo, Y.; Guo, W.; Ngo, H.H.; Nghiem, L.D.; Hai, F.I.; Zhang, J.; Liang, S.; Wang, X.C. A review on the occurrence of micropollutants in the aquatic environment and their fate and removal during wastewater treatment. *Sci. Total Environ.* **2014**, *473*, 619–641. [[CrossRef](#)]
2. Verlicchi, P.; Al Aukidy, M.; Zambello, E. Occurrence of pharmaceutical compounds in urban wastewater: Removal, mass load and environmental risk after a secondary treatment—A review. *Sci. Total. Environ.* **2012**, *429*, 123–155. [[CrossRef](#)] [[PubMed](#)]
3. Petrie, B.; Barden, R.; Kasprzyk-Hordern, B. A review on emerging contaminants in wastewaters and the environment: Current knowledge, understudied areas and recommendations for future monitoring. *Water Res.* **2015**, *72*, 3–27. [[CrossRef](#)] [[PubMed](#)]
4. Ratola, N.; Cincinelli, A.; Alves, A.; Katsoyiannis, A. Occurrence of organic microcontaminants in the wastewater treatment process. A mini review. *J. Hazard. Mater.* **2012**, *239*, 1–18. [[CrossRef](#)]
5. Kidd, K.A.; Blanchfield, P.J.; Mills, K.H.; Palace, V.P.; Evans, R.E.; Lazorchak, J.M.; Flick, R.W. Collapse of a fish population after exposure to a synthetic estrogen. *Proc. Natl. Acad. Sci. USA* **2007**, *104*, 8897–8901. [[CrossRef](#)]
6. Escher, B.I.; Baumgartner, R.; Koller, M.; Treyer, K.; Lienert, J.; McArdell, C.S. Environmental toxicology and risk assessment of pharmaceuticals from hospital wastewater. *Water Res.* **2011**, *45*, 75–92. [[CrossRef](#)]

7. Gadipelly, C.; Pérez-González, A.; Yadav, G.D.; Ortiz, I.; Ibáñez, R.; Rathod, V.K.; Marathe, K.V. Pharmaceutical industry wastewater: Review of the technologies for water treatment and reuse. *Ind. Eng. Chem. Res.* **2014**, *53*, 11571–11592. [[CrossRef](#)]
8. Rodea-Palomares, I.; Gonzalez-Pleiter, M.; Gonzalo, S.; Rosal, R.; Leganes, F.; Sabater, S.; Casellas, M.; Muñoz-Carpena, R.; Fernández-Piñas, F. Hidden drivers of low-dose pharmaceutical pollutant mixtures revealed by the novel GSA-QHTS screening method. *Sci. Adv.* **2016**, *2*, e1601272. [[CrossRef](#)] [[PubMed](#)]
9. Christophoridis, C.; Nika, M.-C.; Aalizadeh, R.; Thomaidis, N.S. Ozonation of ranitidine: Effect of experimental parameters and identification of transformation products. *Sci. Total Environ.* **2016**, *557*, 170–182. [[CrossRef](#)] [[PubMed](#)]
10. European Commission. Directive 2013/39/EU of the European Parliament and of the Council of 12 August 2013 Amending Directives 2000/60/EC and 2008/105/EC as Regards Priority Substances in the Field of Water Policy. *Off. J. Eur. Union* **2013**, *OJL 226*, 1–17.
11. European Commission. Decision (EU) 2015-495 of 20 March 2015 establishing a watch list of substances for Union-wide monitoring in the field of water policy pursuant to Directive 2008/105/EC of the European Parliament and of the Council. *Off. J. Eur. Union* **2015**, *OJL 78*, 40–42.
12. Villota, N.; Lomas, J.M.; Camarero, L.M. Kinetic modelling of water-color changes in a photo-Fenton system applied to oxidate paracetamol. *J. Photochem. Photobiol. A Chem.* **2018**, *356*, 573–579. [[CrossRef](#)]
13. Slamani, S.; Abdelmalek, F.; Ghezzer, M.R.; Addou, A. Initiation of Fenton process by plasma gliding arc discharge for the degradation of paracetamol in water. *J. Photochem. Photobiol. A Chem.* **2018**, *359*, 1–10. [[CrossRef](#)]
14. Akhi, Y.; Irani, M.; Olya, M.E. Simultaneous degradation of phenol and paracetamol using carbon/MWCNT/Fe<sub>3</sub>O<sub>4</sub> composite nanofibers during photo-like-Fenton process. *J. Taiwan Inst. Chem. Eng.* **2016**, *63*, 327–335. [[CrossRef](#)]
15. Abdel-Wahab, A.-M.; Al-Shirbini, A.-S.; Mohamed, O.; Nasr, O. Photocatalytic degradation of paracetamol over magnetic flower-like TiO<sub>2</sub>/Fe<sub>2</sub>O<sub>3</sub> core-shell nanostructures. *J. Photochem. Photobiol. A Chem.* **2017**, *347*, 186–198. [[CrossRef](#)]
16. Augusto, T.D.M.; Chagas, P.; Sangiorgio, D.L.; Leod, T.C.D.O.M.; Oliveira, L.C.; De Castro, C.S. Iron ore tailings as catalysts for oxidation of the drug paracetamol and dyes by heterogeneous Fenton. *J. Environ. Chem. Eng.* **2018**, *6*, 6545–6553. [[CrossRef](#)]
17. Silva, C.P.; Jaria, G.; Otero, M.; Esteves, V.I.; Calisto, V. Waste-based alternative adsorbents for the remediation of pharmaceutical contaminated waters: Has a step forward already been taken? *Bioresour. Technol.* **2018**, *250*, 888–901. [[CrossRef](#)]
18. Mirzaei, A.; Haghghat, F.; Chen, Z.; Yerushalmi, L. Removal of pharmaceuticals from water by homo/heterogeneous Fenton-type processes—A review. *Chemosphere* **2017**, *174*, 665–688. [[CrossRef](#)]
19. Badawy, M.I.; Wahaab, R.A.; El-Kalliny, A. Fenton-biological treatment processes for the removal of some pharmaceuticals from industrial wastewater. *J. Hazard. Mater.* **2009**, *167*, 567–574. [[CrossRef](#)]
20. Velichkova, F.; Julcour-Lebigue, C.; Koumanova, B.; Delmas, H. Heterogeneous Fenton oxidation of paracetamol using iron oxide (nano)particles. *J. Environ. Chem. Eng.* **2013**, *1*, 1214–1222. [[CrossRef](#)]
21. Kalmakhanova, M.S.; Diaz de Tuesta, J.L.; Massalimova, B.K.; Gomes, H.T. Pillared clays from natural resources as catalysts for catalytic wet peroxide oxidation: Characterization and kinetic insights. *Environ. Eng. Res.* **2019**. [[CrossRef](#)]
22. Mnasri-Ghnimi, S.; Frini-Srasra, N. Catalytic wet peroxide oxidation of phenol over Ce-Zr-modified clays: Effect of the pillaring method. *Korean J. Chem. Eng.* **2015**, *32*, 68–73. [[CrossRef](#)]
23. Mnasri-Ghnimi, S.; Frini-Srasra, N. Effect of Al and Ce on Zr-pillared bentonite and their performance in catalytic oxidation of phenol. *Russ. J. Phys. Chem. A* **2016**, *90*, 1766–1773. [[CrossRef](#)]
24. Tomul, F.; Basoglu, F.T.; Canbay, H. Determination of adsorptive and catalytic properties of copper, silver and iron contain titanium-pillared bentonite for the removal bisphenol A from aqueous solution. *Appl. Surf. Sci.* **2016**, *360*, 579–593. [[CrossRef](#)]
25. Galeano, L.-A.; Vicente, M.A.; Gil, A. Catalytic degradation of organic pollutants in aqueous streams by mixed Al/M-pillared clays (M = Fe, Cu, Mn). *Catal. Rev.* **2014**, *56*, 239–287. [[CrossRef](#)]
26. Rhodes, C.N.; Franks, M.; Parkes, G.M.B.; Brown, D.R. The effect of acid treatment on the activity of clay supports for ZnCl<sub>2</sub> alkylation catalysts. *J. Chem. Soc. Chem. Commun.* **1991**, 804–807. [[CrossRef](#)]

27. Yu, W.; Wang, P.; Zhou, C.; Zhao, H.; Tong, D.; Zhang, H.; Yang, H.; Ji, S.; Wang, H. Acid-activated and WO<sub>3</sub>-loaded montmorillonite catalysts and their catalytic behaviors in glycerol dehydration. *Chin. J. Catal.* **2017**, *38*, 1087–1100. [[CrossRef](#)]
28. Cool, P.; Vansant, E.F. Pillared Clays: Preparation, characterization and applications. In *Synthesis*; Springer: Berlin/Heidelberg, Germany, 2001; Volume 1, pp. 265–288.
29. Thommes, M.; Kaneko, K.; Neimark, A.V.; Olivier, J.P.; Rodríguez-Reinoso, F.; Rouquerol, J.; Sing, K.S. Physisorption of gases, with special reference to the evaluation of surface area and pore size distribution (IUPAC Technical Report). *Pure Appl. Chem.* **2015**, *87*, 1051–1069. [[CrossRef](#)]
30. Trigueiro, P.; Pereira, F.A.; Guillermin, D.; Rigaud, B.; Balme, S.; Janot, J.-M.; Dos Santos, I.M.; Fonseca, M.G.; Walter, P.; Jaber, M. When anthraquinone dyes meet pillared montmorillonite: Stability or fading upon exposure to light? *Dyes Pigments* **2018**, *159*, 384–394. [[CrossRef](#)]
31. Sprynskyy, M.; Sokol, H.; Rafińska, K.; Brzozowska, W.; Railean-Plugaru, V.; Pomastowski, P.; Buszewski, B. Preparation of AgNPs/saponite nanocomposites without reduction agents and study of its antibacterial activity. *Colloids Surf. B Biointerfaces* **2019**, *180*, 457–465. [[CrossRef](#)]
32. Zhu, B.-L.; Qi, C.-L.; Zhang, Y.-H.; Bisson, T.; Xu, Z.; Fan, Y.-J.; Sun, Z.-X. Synthesis, characterization and acid-base properties of kaolinite and metal (Fe, Mn, Co) doped kaolinite. *Appl. Clay Sci.* **2019**, *179*, 105138. [[CrossRef](#)]
33. Wu, C.; Wei, X.; Liu, P.; Tan, J.; Liao, C.; Wang, H.; Yin, L.; Zhou, W.; Cui, H.-J. Influence of structural Al species on Cd(II) capture by iron muscovite nanoparticles. *Chemosphere* **2019**, *226*, 907–914. [[CrossRef](#)]
34. Yuan, P.; Annabi-Bergaya, F.; Tao, Q.; Fan, M.; Liu, Z.; Zhu, J.; He, H.; Chen, T. A combined study by XRD, FTIR, TG and HRTEM on the structure of delaminated Fe-intercalated/pillared clay. *J. Colloid Interface Sci.* **2008**, *324*, 142–149. [[CrossRef](#)] [[PubMed](#)]
35. Liu, Y.; Dong, C.; Wei, H.; Yuan, W.; Li, K. Adsorption of levofloxacin onto an iron-pillared montmorillonite (clay mineral): Kinetics, equilibrium and mechanism. *Appl. Clay Sci.* **2015**, *118*, 301–307. [[CrossRef](#)]
36. Widjaya, R.R.; Juwono, A.L.; Rinaldi, N. Bentonite modification with pillarization method using metal stannum. *AIP Conf. Proc.* **2017**, *1904*, 020010.
37. Bahranowski, K.; Włodarczyk, W.; Wisła-Walsh, E.; Gawel, A.; Matusik, J.; Klimek, A.; Gil, B.; Michalik-Zym, A.; Dula, R.; Socha, R.; et al. [Ti,Zr]-pillared montmorillonite—A new quality with respect to Ti- and Zr-pillared clays. *Microporous Mesoporous Mater.* **2015**, *202*, 155–164. [[CrossRef](#)]
38. Bruckman, V.J.; Wriessnig, K. Improved soil carbonate determination by FT-IR and X-ray analysis. *Environ. Chem. Lett.* **2013**, *11*, 65–70. [[CrossRef](#)]
39. Li, T.; Zhao, L.; Zheng, Z.; Zhang, M.; Sun, Y.; Tian, Q.; Zhang, S. Design and preparation acid-activated montmorillonite sustained-release drug delivery system for dexibuprofen in vitro and in vivo evaluations. *Appl. Clay Sci.* **2018**, *163*, 178–185. [[CrossRef](#)]
40. Jain, S.; Datta, M. Montmorillonite-alginate microspheres as a delivery vehicle for oral extended release of Venlafaxine hydrochloride. *J. Drug Deliv. Sci. Technol.* **2016**, *33*, 149–156. [[CrossRef](#)]
41. Komadel, P. Acid activated clays: Materials in continuous demand. *Appl. Clay Sci.* **2016**, *131*, 84–99. [[CrossRef](#)]
42. Eren, E.; Afsin, B. An investigation of Cu(II) adsorption by raw and acid-activated bentonite: A combined potentiometric, thermodynamic, XRD, IR, DTA study. *J. Hazard. Mater.* **2008**, *151*, 682–691. [[CrossRef](#)] [[PubMed](#)]
43. Wang, S.; Dong, Y.; He, M.; Chen, L.; Yu, X. Characterization of GMZ bentonite and its application in the adsorption of Pb(II) from aqueous solutions. *Appl. Clay Sci.* **2009**, *43*, 164–171. [[CrossRef](#)]
44. De Tuesta, J.D.; Quintanilla, A.; Casas, J.; Rodriguez, J. P-, B- and N-doped carbon black for the catalytic wet peroxide oxidation of phenol: Activity, stability and kinetic studies. *Catal. Commun.* **2017**, *102*, 131–135. [[CrossRef](#)]
45. Alalm, M.G.; Tawfik, A.; Ookawara, S. Degradation of four pharmaceuticals by solar photo-Fenton process: Kinetics and costs estimation. *J. Environ. Chem. Eng.* **2015**, *3*, 46–51. [[CrossRef](#)]
46. Trovó, A.G.; Nogueira, R.F.P.; Agüera, A.; Fernández-Alba, A.R.; Malato, S. Paracetamol degradation intermediates and toxicity during photo-Fenton treatment using different iron species. *Water Res.* **2012**, *46*, 5374–5380. [[CrossRef](#)] [[PubMed](#)]
47. De Tuesta, J.L.D.; Silva, A.M.; Faria, J.L.; Gomes, H.T. Removal of Sudan IV from a simulated biphasic oily wastewater by using lipophilic carbon adsorbents. *Chem. Eng. J.* **2018**, *347*, 963–971. [[CrossRef](#)]

48. Diaz de Tuesta, J.L.; Machado, B.F.; Serp, P.; Silva, A.M.T.; Faria, J.L.; Gomes, H.T. Janus amphiphilic carbon nanotubes as Pickering interfacial catalysts for the treatment of oily wastewater by selective oxidation with hydrogen peroxide. *Catal. Today* **2019**. [[CrossRef](#)]



© 2019 by the authors. Licensee MDPI, Basel, Switzerland. This article is an open access article distributed under the terms and conditions of the Creative Commons Attribution (CC BY) license (<http://creativecommons.org/licenses/by/4.0/>).